Research Report

Abnormal microglial–neuronal spatial organization in the dorsolateral prefrontal cortex in autism

John T. Morgan[a,*], **Gursharan Chana**[b], **Ian Abramson**[c], **Katerina Semendeferi**[d], **Eric Courchesne**[a,1], **Ian P. Everall**[b,1]

[a]*Department of Neuroscience, School of Medicine, University of California, San Diego, 9500 Gilman Drive, # 0602, La Jolla, CA 92093-0602, USA*
[b]*Department of Psychiatry, School of Medicine, University of California, San Diego, 9500 Gilman Drive, # 0602, La Jolla, CA 92093-0602, USA*
[c]*Department of Mathematics, University of California, San Diego, 9500 Gilman Drive, # 0112, La Jolla, CA 92093-0112, USA*
[d]*Department of Anthropology, University of California, San Diego, 9500 Gilman Drive, # 0532, La Jolla, CA 92093-0532, USA*

ABSTRACT

Microglial activation and alterations in neuron number have been reported in autism. However, it is unknown whether microglial activation in the disorder includes a neuron-directed microglial response that might reflect neuronal dysfunction, or instead indicates a non-directed, pro-activation brain environment. To address this question, we examined microglial and neuronal organization in the dorsolateral prefrontal cortex, a region of pronounced early brain overgrowth in autism, via spatial pattern analysis of 13 male postmortem autism subjects and 9 controls. We report that microglia are more frequently present near neurons in the autism cases at a distance interval of 25 μm, as well as 75 and 100 μm. Many interactions are observed between near-distance microglia and neurons that appear to involve encirclement of the neurons by microglial processes. Analysis of a young subject subgroup preliminarily suggests that this alteration may be present from an early age in autism. We additionally observed that neuron–neuron clustering, although normal in cases with autism as a whole, increases with advancing age in autism, suggesting a gradual loss of normal neuronal organization in the disorder. Microglia–microglia organization is normal in autism at all ages, indicating that aberrantly close microglia–neuron association in the disorder is not a result of altered microglial distribution. Our findings confirm that at least some microglial activation in the dorsolateral prefrontal cortex in autism is associated with a neuron-specific reaction, and suggest that neuronal organization may degrade later in life in the disorder.

1. Introduction

The alterations in cellular microstructure that underlie macrostructural and functional abnormalities in autism are only beginning to be characterized. Surprisingly, despite the presence of regionally focused early brain overgrowth in some subjects with autism (Carper et al., 2002; Courchesne et al., 2001; Dawson et al., 2007; Dementieva et al., 2005;

* *Corresponding author at:* University of California, Davis M.I.N.D. Institute, 2805 50th St, Sacramento, CA 95817, USA. Fax: +1 916 703 0370.
  E-mail address: jtmorgan61@gmail.com (J.T. Morgan).
 [1] These authors contributed equally to this manuscript.

Please cite this article as: Morgan, J.T., et al., Abnormal microglial–neuronal spatial organization in the dorsolateral prefrontal cortex in autism, Brain Res. (2012), doi:10.1016/j.brainres.2012.03.036

Dissanayake et al., 2006; Hazlett et al., 2005; Redcay and Courchesne, 2005; Schumann et al., 2010; Sparks et al., 2002; Webb et al., 2007), two groups have reported reductions in neuron number in groups comprised primarily of adolescent and adult subjects (Schumann and Amaral, 2006; van Kooten et al., 2008). Abnormalities in neuron organization have been qualitatively reported in a variety of brain regions, but limited subject availability has led to significant variability in the nature and location of the reported alterations (Bailey et al., 1998; Bauman, 1996; Bauman and Kemper, 1994; Kemper and Bauman, 1998). Additionally, a loss of neuropil volume, the space between neurons which is largely composed of neuronal connective elements, has been suggested by minicolumn analyses showing reduced column width, suggestive of possible axonal and dendritic degeneration (Buxhoeveden et al., 2006; Casanova et al., 2002a; Casanova et al., 2006). Despite these prior findings, it has yet to be determined whether there are quantifiable alterations in neuronal organization in the cortex in autism.

In addition to neuronal alterations, changes in microglial morphology and population density that are indicative of activation in autism have been observed (Morgan et al., 2010; Vargas et al., 2005). Normally functioning microglia are known to be intimately involved in supporting, functionally regulating, and if necessary removing aberrantly functioning neurons (Bessis et al., 2005; Christopherson et al., 2005; Ransohoff and Perry, 2009). Therefore, one possibility is that microglial activation in autism reflects or results in

a response to abnormally functioning neurons, whether protective, deleterious, or an attempt to correct abnormal neuronal functioning, perhaps due to altered neuronal connectivity. However, it might instead be the case that the reported alterations reflect alterations in the innate immune system or blood–brain barrier, or genetic immune abnormalities, that produce moderate microglial activation without a neuron-directed response.

To address these questions regarding microglial and neuronal organization, we recorded the cellular co-ordinates of both neurons and ionized calcium-binding adapter molecule-1 (iba-1) positive microglia in the dorsolateral prefrontal cortex (dlPFC), a region of pronounced early macrostructural overgrowth in autism (Carper and Courchesne, 2005). The organization of both neuronal and microglial populations, as well as their interaction, was analyzed in a density-independent, cortical layer-corrected fashion via spatial pattern analysis using the k-function, a technique that has previously been adapted to assess alterations in cellular organization in human postmortem tissue in several
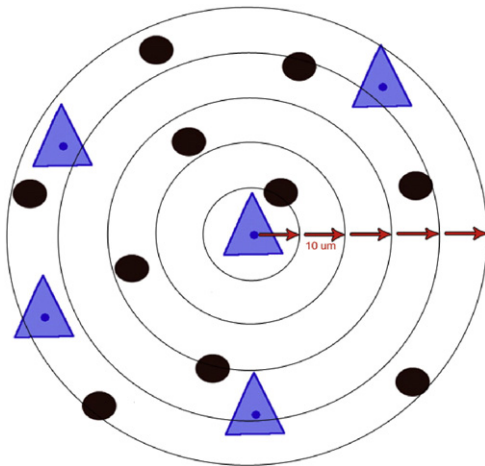

Fig. 1 – Spatial pattern analysis methodology. The number of cells of the population of interest is assessed at distance increments from each analyzed cell. In this example, neurons (blue triangles) and microglia (brown circles) are assessed at distance intervals of 10 μm from a neuron. The population number at each distance interval is compared to 200 simulations in which cell location is randomized by layer in order to produce a density-corrected spatial clustering ratio. Ratios greater than 1 indicate a greater presence of the population of interest (clustering) than would be expected in the spatially randomized condition, while ratios below 1 indicate anti-clustering.
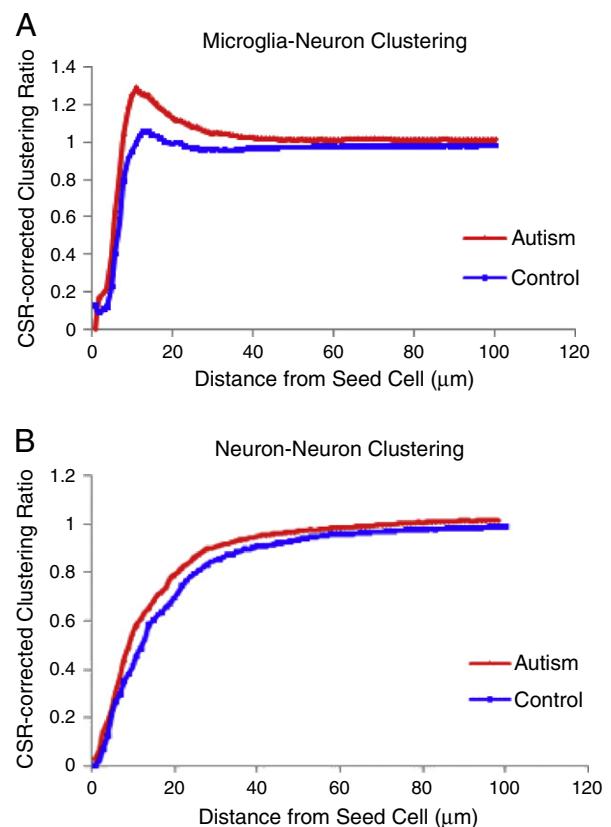

Fig. 2 – Features of cellular spatial clustering over the range of analysis. A. Microglia–neuron interaction is significantly increased in autism at 25 μm (p = .006), 75 μm (p = .005), and 100 μm (p = .005). The profile is marked by a spike in spatial clustering in the 10–30 μm range that is more pronounced in the autism group. B. Neuron–neuron spatial clustering is not significantly different at any distance interval, and lacks prominent features across the distance range in either diagnostic group. Abbreviations: CSR, Complete Spatial Randomness.

clinical disorders (Fig. 1) (Asare et al., 1996; Chana et al., 2003; Diggle and Chetwynd, 1991; Landau and Everall, 2008; Landau et al., 2004; Schladitz et al., 2003).

2. Results

2.1. Microglia–neuron organization

Density-corrected microglia–neuron spatial clustering was significantly increased in the dorsolateral prefrontal cortex of autism subjects relative to control subjects at three of the four a priori selected analysis distance intervals: 25 μm (p=.006), 75 μm (p=.005), and 100 μm (p=.005) (Fig. 2). No significant difference was present at 50 μm (p=.086).

To characterize the nature of this interaction, we qualitatively examined numerous instances of microglia–neuron interaction in the cases showing the highest degree of short-distance clustering. A subset of neurons demonstrated close interactions with microglia, with the center of the microglial nucleus at less than 25 μm from the center of the neuronal nucleus. These interactions not only involved apparent contact between the soma of the microglia and neuron, but frequently included somal encirclement via microglial processes (Fig. 3). Some neurons were also observed to be encircled by microglial processes at a substantial distance from the microglial soma, although this feature was much less common (Fig. 3).

Given the well-established neurodevelopmental basis of autism, we performed a preliminary analysis of a subgroup of young subjects under 6 years of age to capture subjects likely to be displaying early brain growth abnormalities. In this subgroup, effect sizes were very large at the short distance interval 25 μm (1.3), but were less than 0.3 at greater distance intervals. Subject numbers were insufficient (n=3 autism, n=2 control) to perform a formal analysis of group differences.

2.2. Neuron–neuron organization

No significant differences in neuron–neuron organization were present between diagnostic groups (Fig. 2) at any of the a priori selected analysis distance intervals. However, a significant positive correlation between age and neuron–neuron spatial clustering was present within autism subjects specifically at 50 μm (r(13)=.65; p=.016), 75 μm (r(13)=.66; p=.014), and 100 μm (r(13)=.64; p=.018), but not control subjects.

Because of the possible differential developmental profile of neuron–neuron spatial clustering at greater analysis distance intervals (Fig. 4), we performed an exploratory analysis of adults ages 20 and older (n=4 autism; n=6 control) as a subgroup. Significant increases in neuron–neuron spatial clustering were present in adult subjects with autism relative to the age-matched control group at 50 μm (p=.002), 75 μm (p=.006), and 100 μm (p<.001). However, the findings at 50 μm and 75 μm, which were significant via bootstrapping, failed to reach significance via alternate Kolmogorov–Smirnoff test (p=.071; p=.134, respectively). The divergence between significance values in these non-parametric tests may be attributed to the small group size.
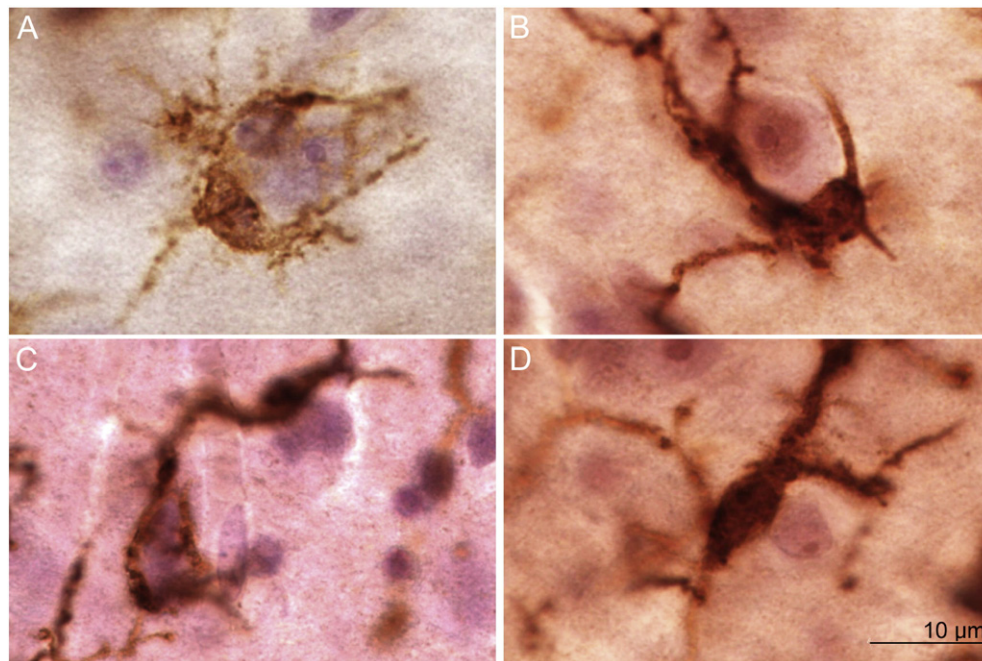

Fig. 3 – Examples of near distance microglia–neuron interaction in subjects with autism. A. Process encirclement of a neighboring neuron in the young subject with autism (BTB-4029) that demonstrated the most markedly increased spatial clustering relative to randomness. B. Processes encircling a neighboring neuron in an adolescent subject with autism (UMB-4899) that demonstrated markedly increased local clustering relative to randomness. C. Processes encircling a neuron at a substantial distance from the microglial soma in UMB-4899. D. An example of a microglial soma adjoining a small neuron without process encirclement in an adult subject with autism (B-5173).
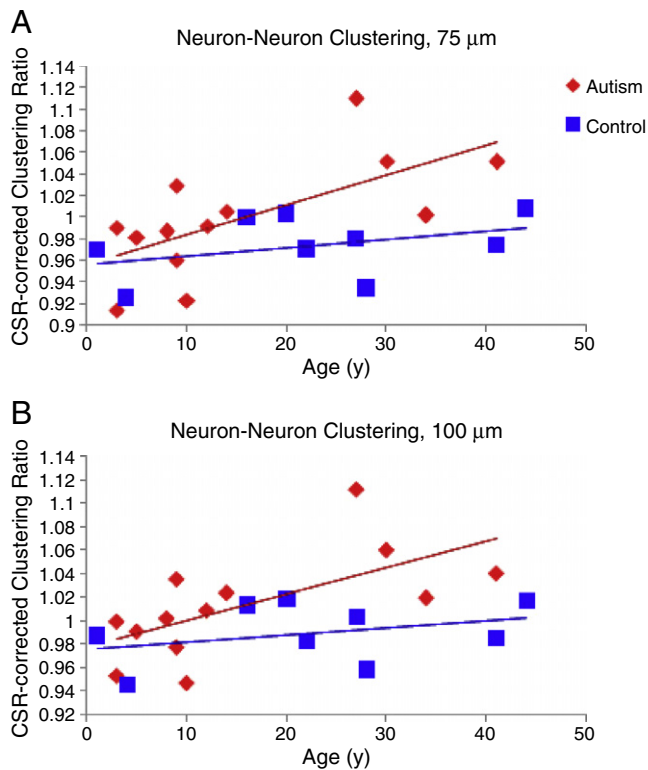
Fig. 4 – Developmental features of neuron–neuron spatial clustering. A. Neuron–neuron spatial clustering at 75 μm, which is significantly correlated with age in autism but not in control subjects. B. Neuron–neuron spatial clustering at 100 μm, which is significantly correlated with age in autism but not in control subjects. Abbreviations: CSR, Complete Spatial Randomness.

2.3. Microglia–microglia organization

No significant differences in microglia–microglia spatial clustering were observed between any diagnostic group or subgroup at any analysis distance (Fig. 5). Microglia–microglia interactions at 50 μm and under were marked by far more substantial spatial anti-clustering than was apparent in either neuron–neuron or microglia–neuron interactions (Fig. 5). Across all subjects as a whole, there was a significant positive correlation between age and microglia–microglia spatial clustering at the shorter analysis distance intervals of 25 μm (r(22) = .70; p < .001) and 50 μm (r(22) = .43; p = .049) (Fig. 5).

3. Discussion

In the dorsolateral prefrontal cortex, microglia–neuron spatial clustering is increased in subjects with autism relative to controls at both local and long distance intervals, indicating neuronal recruitment of a microglial response in the disorder. The morphology associated with this interaction often involves extensive process encirclement, which is reminiscent of several processes observed in vitro but to our knowledge has yet to be described in another neurodevelopmental or neurodegenerative disorder. Thus, it is unclear at present exactly

what process this interaction reflects. The microglia could be responsible for protective, pro-healing, or deleterious effects on neuronal health. They could also be tasked with correcting abnormal neuronal connectivity and functioning via synaptic interaction (Hutsler and Zhang, 2010; Wake et al., 2009). The presence of a specific interaction between these cellular populations is, however, strong evidence against two possibilities. One is that prior reports of microglial activation in autism (Morgan et al., 2010; Vargas et al., 2005) reflect primarily broad systemic alterations in innate immune function not driven by other cellular abnormalities in the brain. The other is that microglial activation primarily reflects the presence of perimortem activation. This finding is also strongly congruent with recent data indicating that glial activation in autism may lack a strong genetic basis and/or be secondary to neuronal alterations in the disorder (Voineagu et al., 2011).

A few details of the microglia–neuron spatial clustering profile deserve additional comment. One is the absence of significant group difference at 50 μm. This may reflect a local deficit of microglia moving out of this intermediate-distance range nearer to neurons, while at distances greater than 50 μm milder attractive mechanisms predominate. Another feature of note is that the increase in microglia–neuron
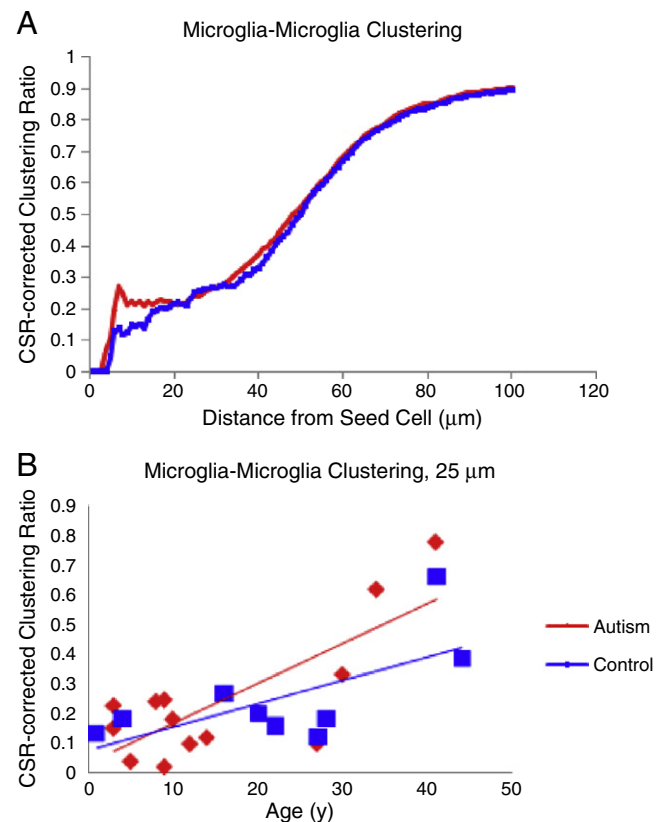

Fig. 5 – Features of microglia–microglia interaction. A. Microglia–microglia interactions in both autism and control subjects. Strong anti-clustering is present at near distances in both autism and control subjects. No group differences are present. B. Developmental microglia–microglia organization. Local anti-clustering is reduced with increasing age in both autism and control subjects. Abbreviations: CSR, Complete Spatial Randomness.

clustering in autism preliminarily appears to be present in the youngest subjects studied. These few subjects are from an age range during which early brain overgrowth may be occurring in the dorsolateral prefrontal cortex. This is also a period in which abnormal function may be emerging, suggesting that aberrant microglia–neuron interaction may reflect or be involved in the development of the disorder in some subjects. However, the consistency of group differences when age is considered as a covariate suggests that that the interaction between these cellular populations remains abnormal across the lifespan.

Of particular interest is the frequent presence of extensive microglial processes encircling the neuronal soma. Similar alterations have been observed during axonal regrowth in the peripheral nervous system (Shokouhi et al., 2010; Svensson et al., 1994) and brainstem (Kalla et al., 2001), as well as in instances of focal inflammation in the CNS (Trapp et al., 2007). These closely associated microglia may also be engaged in synaptic stripping or other forms of synaptic remodeling in response to aberrant neuronal connectivity (Blinzinger and Kreutzberg, 1968; Kreutzberg, 1996), actions often considered protective towards aberrantly functioning neurons (Trapp et al., 2007). An increase in microglia–neuron interaction could also reflect removal of dying or damaged neurons, or extension of trophic support to compromised neurons (Bessis et al., 2007; Christopherson et al., 2005; Davoust et al., 2008; Ransohoff and Perry, 2009). However, there remains the possibility that increased microglia–neuron interaction may also be deleterious, reflecting excessive and perhaps damaging interaction with neurons. This activation might occur in response to autoimmunity or other sources of pro-inflammatory signaling (Ahlsen et al., 1993; Garbett et al., 2008; Gupta et al., 1998; Jyonouchi et al., 2001; Laurence and Fatemi, 2005; Li et al., 2009; Singh et al., 1991; Vargas et al., 2005; Zimmerman et al., 2005).

3.1. Neuron–neuron spatial clustering is increased in older subjects with autism

No significant differences in neuronal organization were present between autism and control cases as a whole, but a significant reduction in neuron–neuron anti-clustering was observed with increasing age in autism at greater analysis distances. This alteration may reflect the statistical aggregation of many minor alterations in neuronal organization rather than direct near-distance cellular interactions, as appears to be the case in the microglia–neuron interaction. The source of these additive alterations is unclear, but it appears reasonable to suggest that it may reflect a haphazard loss of neurons and/or neuronal connective elements (neuropil) in the dorsolateral prefrontal cortex. This finding is consonant with prior findings of reduced neuron number (Schumann and Amaral, 2006; van Kooten et al., 2008), reduced dendritic arbor volume (Raymond et al., 1996), and reduced neuropil volume between neuronal minicolumns (Buxhoeveden et al., 2006; Casanova et al., 2002b; Casanova et al., 2006) in groups of older children, adolescents, adults, and age-unsegregated subjects with autism. It is of note that these studies that have largely focused on other regions of the brain, but regions that also demonstrate early overgrowth in some subjects. Reductions in cortical thickness with increasing age have also been reported in

autism (Hutsler et al., 2007), as well as increases in spine density in adolescents and adults that might produce unusual connectivity and organization (Hutsler and Zhang, 2010). The preliminary finding of absence of neuronal organization changes in younger subjects with autism suggests that in most subjects there may be either no early alteration in neuronal properties such as proliferation or connectivity, or that any early alteration in neuronal proliferation or connectivity happens in a relatively uniform fashion, reflecting processes that are relatively consistent from cell to cell. However, a qualitative examination of individual subjects also suggests the possibility that a few young subjects may demonstrate modest disorganization relative to controls. Additional pediatric cases must be examined to determine whether there are early changes in neuronal organization in some cases with autism.

3.2. Microglia–microglia interactions are normal in autism and marked by strong anti-clustering

Microglia–microglia interactions in the dorsolateral prefrontal cortex do not significantly differ between subjects with autism and controls. This indicates that the alterations in microglia–neuron interaction we report cannot be accounted for by alterations in microglial organization alone. This data also suggests that the genetic and environmental factors governing the spatial organization of microglia are likely unaffected in autism. The strong, consistent local repulsion we observe in all subjects is further evidence that specific, small volumes within the brain are monitored by individual microglial cells, as suggested by prior in vitro experiments (Nimmerjahn et al., 2005; Ransohoff and Perry, 2009). A surprising finding is our observation of a striking breakdown in local microglia–microglia spatial anti-clustering by middle age regardless of diagnosis. This alteration should be examined in this brain region in a middle-aged to elderly control cohort as a possible precursor to glial dysregulation and neurodegeneration late in life.

In summary, our findings suggest that the dorsolateral prefrontal cortex in autism exhibits increased short-distance microglia–neuron interaction, including encirclement of neurons by microglial processes. Therefore, microglial activation in autism likely reflects some neuron-directed processes in at least some regions of the brain. Additionally, neuron–neuron organization appears to be grossly normal in the dorsolateral prefrontal cortex in autism but there may be alterations that emerge over the lifespan, with neuron or neuropil loss strong possible explanations. Finally, microglia–microglia organization is normally maintained in the dorsolateral prefrontal cortex in autism despite the presence of microglial activation, but the even spacing of microglia shows a remarkable degradation by middle age in both autism and control subjects that may be a precursor to neurodegenerative events. Future studies should investigate whether the abnormalities we observe are present from early in development in autism. It will also be important to determine whether they are consistent across the brain, vary depending on whether the examined region shows early overgrowth and/or dysfunction in some subjects, or are limited to a few cortical regions. Most critical will be to determine the specific nature of microglia–neuron interactions in autism.

This knowledge may hold important clues to abnormalities in both immune and neuronal functioning in the disorder.

4. Experimental procedures

4.1. Tissue acquisition and processing

Formalin-fixed tissue with a minimum of 1 year fixation time was acquired from the dlPFC of n=13 autism and n=9 control subjects. Individual subject information is provided in Table 1. 10/13 cases were diagnosed with autism via the Autism Diagnostic Interview-Revised. The remaining 3 cases were diagnosed based on written descriptions from unscored Pre-Linguistic Autism Diagnostic Observation Schedule, Childhood Autism Rating Scale, or multiple neurology reports with detail sufficient to conclude the case met full Diagnostic and Statistical Manual-IV criteria for autism. No Asperger's syndrome or Pervasive Developmental Disorder —

Not Otherwise Specified cases were included. The autism group was comprised of all male subjects with suitable dlPFC tissue available for histology from the national brain banks and the Courchesne laboratory collection. The control group was comprised of all suitable adolescent and younger male subjects that were available as well as a numerical match for n=6 adults with autism over 20 years of age. N=2 adult autism subjects were subsequently removed due to concerns regarding comorbid conditions. Five of the autism subjects had been previously assessed for glial abnormality, but this overlap was incidental; subjects were not selected via consideration of the findings of that study (Vargas et al., 2005).

Tissue processing for n=7 subjects (n=4 autism and n=3 control; "NSA" processing in Table 1) was performed by Dr. Robert Switzer (Neuroscience Associates, Knoxville, TN) as follows: whole hemispheres were cryoprotected in 20% glycerol–2% DMSO for 1 week, then cast in a gelatin matrix that was cured for 4 days. The block containing the brain was rapidly

Table 1 – Descriptive information for all subjects. Medication history: [a]Medical records unavailable; [b]Zyprexa, Reminyl, Adderall; [c]Fluvoxamine, Tegretol, Ritalin, Clonidine, Pondimin, Prozac, Luvox, Risperidal; [d]Desipramine; [e]Clonidine; [f]Ritalin, Clonidine; [g]Trileptal, Zoloft, Clonidine, Melatonin; [h]Phenobarbital, Mysoline, Dilantin, Diamox, Zarotin, Tegretol, Diazepam, Clonazepam, Depokene, Tranxene, Cisapride, Valproic Acid; [i]Tegretol, Risperidal, Zyprexa, Melaril, Luvox, Depakote; [j]Tegretol, Epival, Cogentin, Zyprexa, Loxepac, Flurazepam, Synthroid, Dalmane, Stelazine, Nozinan, Rivotril, Chloral Hydrate, Largactil, Kemadrin, Haldol, Procyclidine, Ativan, Lithium, Risperdal, Anafranil, Sulfate Ferreux. Abbreviations: N/A, not available. Brain mass reflects fresh brain weight at autopsy. The 1815 g control brain was confirmed via reference to multiple MRI scans taken during life to not reflect postmortem edema.

Subject number	Diagnosis (ADI-R)	Age	Processing location	Hemisphere	Brain mass (g)	PMI (h)	Fixation time (mo)	Cause of death	Seizure history	Clinical history
BTB-4021	Autism	3	NSA	Left	1330	15	52	Drowning	No	None
BTB-4029	Autism	3	NSA	Left	1130	13	51	Drowning	N/A	None
UMB-1349	Autism	5	UCSD	Right	1620	39	80	Drowning	No	Obesity, undescended testicle
UMB-4231[b]	Autism	8	UCSD	Right	1570	12	41	Drowning	No	None
B-4925[c]	Autism	9	UCSD	Right	1320	27	90	Seizure	Yes	Venous angioma in frontal lobe, chronic middle ear disease
UMB-797[d]	Autism	9	UCSD	Right	1500	13	125	Drowning	No	Chronic migraine
BTB-2004[e]	Autism	10	UCSD	Left	N/A	23	126	Drowning	No	Chronic ear infection
BTB-3878[f]	Autism	12	UCSD	Right	1630	23	60	Drowning	N/A	Moderate hypotonia
UMB-4899[g]	Autism	14	UCSD	Right	N/A	9	16	Drowning	Yes	None
BTB-3663[a]	Autism	27	UCSD	Right	1420	30	84	Neuroleptic malignant syndrome	Yes	None reported
B-5173[h]	Autism	30	UCSD	Right	1230	20	81	GI bleeding	Yes	Scoliosis, gastric Polyp
CAL-101[i]	Autism	34	NSA	Left	1367	17	126	Adult respiratory distress syndrome	Yes	Pneumonia
CAL-104[j]	Autism	41	NSA	Left	1385	N/A	74	Food aspiration	Yes	None
BTB-3958	Control	1	NSA	Left	N/A	24	57	N/A	No	None
UMB-4670	Control	4	UCSD	Right	N/A	17	30	Commotio cordis	No	None
UMB-1796	Control	16	NSA	Right	1440	16	53	Multiple injuries	No	None
UMB-1649	Control	20	UCSD	Right	N/A	22	62	N/A	No	None
B-6221	Control	22	UCSD	Right	1535	24	N/A	N/A	No	None
UMB-818	Control	27	UCSD	Right	N/A	10	121	Multiple injuries	No	None
B-5873	Control	28	UCSD	Right	1580	23	N/A	N/A	No	None
B-5813	Control	41	UCSD	Right	1815	27	N/A	N/A	No	None
BTB-3859	Control	44	NSA	Right	1640	30	62	N/A	No	None

frozen in a mixture of dry ice and 2% methyl butane. The frozen block was mounted and sectioned in the coronal plane at 80 μm.

Tissue processing for n=15 subjects (n=9 autism and n=6 control; "UCSD" processing in Table 1) was carried out at the University of California, San Diego as follows: small blocks of formalin-fixed tissue with an approximate average size of 2×2×1 cm were acquired from dlPFC. The tissue was cryoprotected in 10% sucrose–.1% DMSO for 2 days, followed by 20% sucrose /–.1% DMSO for 2 days, then sectioned at 50 μm on a freezing microtome and stored in cryoprotectant at −20 °C.

4.2.   Tissue preparation

Sections from each of the n=15 UCSD subjects were processed alongside individual gyri isolated from the dlPFC of the n=7 NSA coronal sections with a straightedge razor. All tissue was washed, slide mounted, and air dried for two nights. Immunohistochemistry was performed as follows: peroxidase activity was blocked via 30 minute exposure to 3% H_2O_2 in MeOH. The slides were microwaved in simmering antigen retrieval citra (Biogenex, San Ramon, CA) for 10 min, followed by a 30 minute cooldown. The tissue was blocked and permeabilized with a solution of 5% NGS and .1% Triton X-100 in TBS for 3 h. Incubation with the rabbit polyclonal primary antibody to iba-1 (Wako USA, Richmond, VA) was carried out at 1:1000 concentration in .1% Triton X-100 in TBS for 40 h at 4 °C. The sections were then incubated in anti-rabbit secondary antibody prepared as described from ABC reagent kit (Vector Laboratories, Burlingame, CA) for 2 h, followed by 2 h in ABC reagent. The sections were developed using DAB (Vector Laboratories) as chromogen with a 12 minute exposure time. Finally, the sections were counterstained with hematoxylin/eosin (Vector Laboratories) for 7 min, dehydrated through a progressive series of 70%/95%/100%/100% EtOH (3 min each) and 2 100% xylene (20 min) rinses, and coverslipped with Permount.

4.3.   Data acquisition

Localization to Brodmann Area (BA) 9/46 was confirmed using rigorous cytoarchitectonic criteria (Petrides and Pandya, 1994; Rajkowska and Goldman-Rakic, 1995), with a subset of definitions confirmed by a second observer with expertise in frontal cortical cytoarchitecture (K.S.).

Data was acquired on a Nikon Eclipse 80i microscope (Nikon Instruments, Melville, NY) with a MicroBrightField cx9000 camera (MBF Bioscience, Williston, VT) through a 1.4 N.A. 100× lens in the presence of Köhler illumination. For each subject, a rectangular ROI 600 μm or more in width, extending from pial surface to white matter, and located on the high gyral wall was assessed. The x,y-coordinates of the center of the nuclei of all neurons and microglia in this region were recorded in Stereo Investigator (MBF Bioscience) from an area 8 μm in depth, with a 2 μm guard zone, by a rater blind to subject identity (J.M.). Field depth was selected to ensure consistent iba-1 antibody penetration and approximate the 2-d recordings performed in previous thin-section spatial pattern experiments.

Hematoxylin/eosin stained neurons were distinguished from glial nuclei on the basis of large cell size, the presence of a large nucleus with a visible rim of surrounding cytoplasm, and the presence of a distinct nucleolus. Microglia were distinguished from other glia on the basis of iba-1 staining, which was robust and highly specific for microglia and macrophages in both diagnostic groups, as expected from prior immunostaining experiments performed by the manufacturer. Juxtavascular and perivascular microglia were distinguished from non-parencyhmal iba-1 positive perivascular macrophages on the basis of the rod-shaped morphology of the perivascular macrophages and their alignment with a blood vessel (visible via counterstain).

4.4.   Data analysis

Neuron–neuron spatial clustering, microglia–neuron spatial clustering, and microglia–microglia spatial clustering were assessed via the k-function (Cotter et al., 2002; Diggle and Chetwynd, 1991; Landau et al., 2004) (Fig. 1). Briefly, the number of observations of the target cell type at intervals of 1 μm from each analysis cell was recorded, and these numbers were then summed across all analysis cells. This value was then density-corrected to an individual spatial clustering ratio relative to randomness at each distance interval. This calculation was performed via comparison for each subject to 200 simulations in which equivalent cell density was maintained but the location of the cells was randomized (Diggle and Chetwynd, 1991). Within each subject, our simulations set cell density independently for each layer, allowing correction for variable layer thickness and cellular density properties between subjects. This methodology allowed correction for artifacts that might be present due to differential tissue processing, fixation, and shrinkage between cases. A spatial clustering ratio of one therefore indicates a completely random distribution of cells in a subject, while a spatial clustering ratio greater than one indicates increased clustering relative to spatial randomness and a ratio less than one indicates anti-clustering, or a lattice-like organization, relative to spatial randomness.

Layer boundaries were assigned for each subject by a blind rater (J.M.) based on a reconstruction of neuronal coordinates in Stereo Investigator. The locations of analyzed cells and the maximum analysis range were set so as to avoid ROI edge effects; analyzed cells were limited to 100 μm from the boundary of the ROI and the maximum analysis range was set at 100 μm. Evenly-spaced distance intervals of interest at 25, 50, 75, and 100 μm were selected a priori. Analysis intervals of 125 and 150 μm were also explored, but a lack of interaction effects relative to randomness was observed across all diagnostic groups and cell comparison conditions.

4.5.   Assessment of potential covariates

All group comparisons and correlation analyses were conducted in PASW 18.0 (SPSS Inc., Chicago, IL) unless otherwise noted. All potential confounds and covariates for which there was reliable information available in n=14 or more subjects were examined.

Processing location/section thickness was investigated as a potential confound. No significant or trend interaction effects were observed for processing location for either microglia–neuron or neuron–neuron spatial clustering. A trend was present towards a correlation between processing location and microglia–microglia spatial clustering at 25 μm ($r_{pb}(22) = .42$; $p = .055$) across all subjects as a whole and was significant in the autism subgroup ($r_{pb}(13) = .63$; $p = .022$). However, the correlation between age and microglia–microglia spatial clustering we report in the results remained significant after correction for processing location both across all subjects as a whole ($pr_{pb}(19) = .73$; $p < .001$) and in the autism subgroup ($pr_{pb}(10) = .82$; $p = .001$). Hemisphere could not be examined as a separate covariate due to colinearity with processing location ($r(25) = .72$; $p < .001$).

The groups did not significantly differ by age ($t(20) = 1.16$; $p = .26$). Age and fixation time were examined as covariates and were found to be associated with microglia–neuron spatial clustering at 25 μm specifically. However, we were not able to perform non-parametric bootstrap analyses with age or fixation time as covariates. Via parametric analyses, we verified that adding age and/or fixation time as covariates either increased or did not affect the significance of our findings at all distance intervals in all cellular interactions assessed.

No significant correlation was found between spatial clustering ratios and seizure or postmortem interval, either across all subjects as a whole or within any diagnostic subgroup in any cell comparison condition (see Results). Insufficient data was available to examine a correlation with brain pH or any cognitive measures.

Due to a potential interaction with diagnosis, brain mass was not assessed as a covariate, but was assessed independently for interaction effects. Within all subjects as a whole, there was a trend correlation between age and brain mass ($r(22) = .42$; $p = .051$). This correlation was highly significant in control subjects ($r(9) = .95$; $p < .001$), with a trend correlation in autism subjects ($r(12) = −.60$; $p = .052$). No findings of correlation between brain mass and any outcome measure retained significance after correction for age.

4.6. Non-parametric statistical analysis

Spatial clustering ratios were confirmed to fail the Shapiro–Wilk test for normality in the autism group at all major distance intervals in the microglia–neuron comparison. Therefore, group differences were assessed via non-parametric bootstrapping (Landau and Everall, 2008; Landau et al., 2004) in Matlab R2009b (The Mathworks, Natick, MA). Assessments were performed at every 25 μm within the analysis range, with 100,000 resamples per bootstrap. The results were fitted to a bias-corrected and accelerated (BCa) curve. Repetition revealed variability of $p = .002$ or less between bootstrapping runs. Findings regarding significance were confirmed via two additional non-parametric tests, the Independent-Samples Kolmogorov–Smirnoff and the Mann–Whitney U; the single disagreement regarding significance between the three analysis methodologies is noted in the results. Effect sizes for a young subject subgroup were calculated via Cohen's d at a confidence level of 95%.

REFERENCES

Ahlsen, G., Rosengren, L., Belfrage, M., Palm, A., Haglid, K., Hamberger, A., Gillberg, C., 1993. Glial fibrillary acidic protein in the cerebrospinal fluid of children with autism and other neuropsychiatric disorders. Biol. Psychiatry 33, 734–743.

Asare, E., Dunn, G., Glass, J., McArthur, J., Luthert, P., Lantos, P., Everall, I., 1996. Neuronal pattern correlates with the severity of human immunodeficiency virus-associated dementia complex. Usefulness of spatial pattern analysis in clinicopathological studies. Am. J. Pathol. 148, 31–38.

Bailey, A., Luthert, P., Dean, A., Harding, B., Janota, I., Montgomery, M., Rutter, M., Lantos, P., 1998. A clinicopathological study of autism. Brain 121, 889–905.

Bauman, M., 1996. Neuroanatomic observations of the brain in pervasive developmental disorders. J. Autism Dev. Disord. 26, 199–203.

Bauman, M.L., Kemper, T.L., 1994. Neuroanatomic observations of the brain in autism. Vol. In: Bauman, M.L., Kemper, T.L. (Eds.), The Neurobiology of Autism. Johns Hopkins UP, Baltimore, pp. 119–145.

Bessis, A., Bernard, D., Triller, A., 2005. Tumor necrosis factor-alpha and neuronal development. Neuroscientist 11, 277–281.

Bessis, A., Bechade, C., Bernard, D., Roumier, A., 2007. Microglial control of neuronal death and synaptic properties. Glia 55, 233–238.

Blinzinger, K., Kreutzberg, G., 1968. Displacement of synaptic terminals from regenerating motoneurons by microglial cells. Z. Zellforsch. Mikrosk. Anat. 85, 145–157.

Buxhoeveden, D.P., Semendeferi, K., Buckwalter, J., Schenker, N., Switzer, R., Courchesne, E., 2006. Reduced minicolumns in the frontal cortex of patients with autism. Neuropathol. Appl. Neurobiol. 32, 483–491.

Carper, R.A., Courchesne, E., 2005. Localized enlargement of the frontal cortex in early autism. Biol. Psychiatry 57, 126–133.

Carper, R.A., Moses, P., Tigue, Z.D., Courchesne, E., 2002. Cerebral lobes in autism: early hyperplasia and abnormal age effects. Neuroimage 16, 1038–1051.

Casanova, M.F., Buxhoeveden, D.P., Brown, C., 2002a. Clinical and macroscopic correlates of minicolumnar pathology in autism. J. Child Neurol. 17, 692–695.

Casanova, M.F., Buxhoeveden, D.P., Switala, A.E., Roy, E., 2002b. Minicolumnar pathology in autism. Neurology 58, 428–432.

Casanova, M.F., van Kooten, I.A., Switala, A.E., van Engeland, H., Heinsen, H., Steinbusch, H.W., Hof, P.R., Trippe, J., Stone, J., Schmitz, C., 2006. Minicolumnar abnormalities in autism. Acta Neuropathol (Berl) 112, 287–303.

Chana, G., Landau, S., Beasley, C., Everall, I.P., Cotter, D., 2003. Two-dimensional assessment of cytoarchitecture in the anterior cingulate cortex in major depressive disorder, bipolar disorder, and schizophrenia: evidence for decreased neuronal somal size and increased neuronal density. Biol. Psychiatry 53, 1086–1098.

Christopherson, K.S., Ullian, E.M., Stokes, C.C., Mullowney, C.E., Hell, J.W., Agah, A., Lawler, J., Mosher, D.F., Bornstein, P., Barres, B.A., 2005. Thrombospondins are astrocyte-secreted proteins that promote CNS synaptogenesis. Cell 120, 421–433.

Cotter, D., Landau, S., Beasley, C., Stevenson, R., Chana, G., MacMillan, L., Everall, I., 2002. The density and spatial distribution of GABAergic neurons, labelled using calcium binding proteins, in the anterior cingulate cortex in major depressive disorder, bipolar disorder, and schizophrenia. Biol. Psychiatry 51, 377–386.

Courchesne, E., Karns, C., Davis, H.R., Ziccardi, R., Carper, R., Tigue, Z., Pierce, K., Moses, P., Chisum, H.J., Lord, C., Lincoln, A.J., Pizzo, S., Schreibman, L., Haas, R.H., Akshoomoff, N., Courchesne, R.Y., 2001. Unusual brain growth patterns in early life in patients with autistic disorder: an MRI study. Neurology 57, 245–254.

Davoust, N., Vuaillat, C., Androdias, G., Nataf, S., 2008. From bone marrow to microglia: barriers and avenues. Trends Immunol. 29, 227–234.

Dawson, G., Munson, J., Webb, S.J., Nalty, T., Abbott, R., Toth, K., 2007. Rate of head growth decelerates and symptoms worsen in the second year of life in autism. Biol. Psychiatry 61, 458–464.

Dementieva, Y.A., Vance, D.D., Donnelly, S.L., Elston, L.A., Wolpert, C.M., Ravan, S.A., DeLong, G.R., Abramson, R.K., Wright, H.H., Cuccaro, M.L., 2005. Accelerated head growth in early development of individuals with autism. Pediatr. Neurol. 32, 102–108.

Diggle, P.J., Chetwynd, A.G., 1991. Second-order analysis of spatial clustering for inhomogeneous populations. Biometrics 47, 1155–1163.

Dissanayake, C., Bui, Q.M., Huggins, R., Loesch, D.Z., 2006. Growth in stature and head circumference in high-functioning autism and Asperger disorder during the first 3 years of life. Dev. Psychopathol. 18, 381–393.

Garbett, K., Ebert, P.J., Mitchell, A., Lintas, C., Manzi, B., Mirnics, K., Persico, A.M., 2008. Immune transcriptome alterations in the temporal cortex of subjects with autism. Neurobiol. Dis. 30, 303–311.

Gupta, S., Aggarwal, S., Rashanravan, B., Lee, T., 1998. Th1- and Th2-like cytokines in CD4+ and CD8+ T cells in autism. J. Neuroimmunol. 85, 106–109.

Hazlett, H.C., Poe, M., Gerig, G., Smith, R.G., Provenzale, J., Ross, A., Gilmore, J., Piven, J., 2005. Magnetic resonance imaging and head circumference study of brain size in autism: birth through age 2 years. Arch. Gen. Psychiatry 62, 1366–1376.

Hutsler, J.J., Zhang, H., 2010. Increased dendritic spine densities on cortical projection neurons in autism spectrum disorders. Brain Res. 1309, 83–94.

Hutsler, J.J., Love, T., Zhang, H., 2007. Histological and magnetic resonance imaging assessment of cortical layering and thickness in autism spectrum disorders. Biol. Psychiatry 61, 449–457.

Jyonouchi, H., Sun, S., Le, H., 2001. Proinflammatory and regulatory cytokine production associated with innate and adaptive immune responses in children with autism spectrum disorders and developmental regression. J. Neuroimmunol. 120, 170–179.

Kalla, R., Liu, Z., Xu, S., Koppius, A., Imai, Y., Kloss, C.U., Kohsaka, S., Gschwendtner, A., Moller, J.C., Werner, A., Raivich, G., 2001. Microglia and the early phase of immune surveillance in the axotomized facial motor nucleus: impaired microglial activation and lymphocyte recruitment but no effect on neuronal survival or axonal regeneration in macrophage-colony stimulating factor-deficient mice. J. Comp. Neurol. 436, 182–201.

Kemper, T., Bauman, M., 1998. Neuropathology of infantile autism. J. Neuropathol. Exp. Neurol. 57, 645–652.

Kreutzberg, G.W., 1996. Microglia: a sensor for pathological events in the CNS. Trends Neurosci. 19, 312–318.

Landau, S., Everall, I.P., 2008. Nonparametric bootstrap for k-functions arising from mixed-effects models with applications in neuropathology. Stat. Sin. 18, 1375–1393.

Landau, S., Rabe-Hersketh, S., Everall, I.P., 2004. Nonparametric one-way analysis of variance of replicated bivariate spatial point patterns. Biom. J. 46, 19–34.

Laurence, J.A., Fatemi, S.H., 2005. Glial fibrillary acidic protein is elevated in superior frontal, parietal and cerebellar cortices of autistic subjects. Cerebellum 4, 206–210.

Li, X., Chauhan, A., Sheikh, A.M., Patil, S., Chauhan, V., Li, X.M., Ji, L., Brown, T., Malik, M., 2009. Elevated immune response in the brain of autistic patients. J. Neuroimmunol. 207, 111–116.

Morgan, J.T., Chana, G., Pardo, C.A., Achim, C., Semendeferi, K., Buckwalter, J., Courchesne, E., Everall, I.P., 2010. Microglial activation and increased microglial density observed in the dorsolateral prefrontal cortex in autism. Biol. Psychiatry. 68, 368–376.

Nimmerjahn, A., Kirchhoff, F., Helmchen, F., 2005. Resting microglial cells are highly dynamic surveillants of brain parenchyma in vivo. Science 308, 1314–1318.

Petrides, M., Pandya, D.N., 1994. Comparative architectonic analysis of the human and the macaque frontal cortex. In: Boller, F., Grafman, J. (Eds.), Handbook of Neuropsychology, Vol. 9. Elsevier Science Ltd, Amsterdam, pp. 17–58.

Rajkowska, G., Goldman-Rakic, P.S., 1995. Cytoarchitectonic definition of prefrontal areas in the normal human cortex: I. Remapping of areas 9 and 46 using quantitative criteria. Cereb. Cortex 5, 307–322.

Ransohoff, R.M., Perry, V.H., 2009. Microglial physiology: unique stimuli, specialized responses. Annu. Rev. Immunol. 27, 119–145.

Raymond, G.V., Bauman, M.L., Kemper, T.L., 1996. Hippocampus in autism: a Golgi analysis. Acta Neuropathol. 91, 117–119.

Redcay, E., Courchesne, E., 2005. When is the brain enlarged in autism? A meta-analysis of all brain size reports. Biol. Psychiatry 58, 1–9.

Schladitz, K., Sarkka, A., Pavenstadt, I., Haferkamp, O., Mattfeldt, T., 2003. Statistical analysis of intramembranous particles using freeze fracture specimens. J. Microsc. 211, 137–153.

Schumann, C.M., Amaral, D.G., 2006. Stereological analysis of amygdala neuron number in autism. J. Neurosci. 26, 7674–7679.

Schumann, C.M., Bloss, C.S., Barnes, C.C., Wideman, G.M., Carper, R.A., Akshoomoff, N., Pierce, K., Hagler, D., Schork, N., Lord, C., Courchesne, E., 2010. Longitudinal magnetic resonance imaging study of cortical development through early childhood in autism. J. Neurosci. 30, 4419–4427.

Shokouhi, B.N., Wong, B.Z., Siddiqui, S., Lieberman, A.R., Campbell, G., Tohyama, K., Anderson, P.N., 2010. Microglial responses around intrinsic CNS neurons are correlated with axonal regeneration. BMC Neurosci. 11, 13.

Singh, V.K., Warren, R.P., Odell, J.D., Cole, P., 1991. Changes of soluble interleukin-2, interleukin-2 receptor, T8 antigen, and interleukin-1 in the serum of autistic children. Clin. Immunol. Immunopathol. 61, 448–455.

Sparks, B.F., Friedman, S.D., Shaw, D.W., Aylward, E., Echelard, D., Artru, A.A., Maravilla, K.R., Giedd, J.N., Munson, J., Dawson, G., Dager, S.R., 2002. Brain sructural abnormalities in young children with autism spectrum disorder. Neurology 59, 184–192.

Svensson, M., Eriksson, P., Persson, J., Liu, L., Aldskogius, H., 1994. Functional properties of microglia following peripheral nerve injury. Neuropathol. Appl. Neurobiol. 20, 185–187.

Trapp, B.D., Wujek, J.R., Criste, G.A., Jalabi, W., Yin, X., Kidd, G.J., Stohlman, S., Ransohoff, R., 2007. Evidence for synaptic stripping by cortical microglia. Glia 55, 360–368.

van Kooten, I.A., Palmen, S.J., von Cappeln, P., Steinbusch, H.W., Korr, H., Heinsen, H., Hof, P.R., van Engeland, H., Schmitz, C., 2008. Neurons in the fusiform gyrus are fewer and smaller in autism. Brain 131, 987–999.

Vargas, D.L., Nascimbene, C., Krishnan, C., Zimmerman, A.W., Pardo, C.A., 2005. Neuroglial activation and neuroinflammation in the brain of patients with autism. Ann. Neurol. 57, 67–81.

Voineagu, I., Wang, X., Johnston, P., Lowe, J.K., Tian, Y., Horvath, S., Mill, J., Cantor, R.M., Blencowe, B.J., Geschwind, D.H., 2011. Transcriptomic analysis of autistic brain reveals convergent molecular pathology. Nature 474, 380–384.

Wake, H., Moorhouse, A.J., Jinno, S., Kohsaka, S., Nabekura, J., 2009. Resting microglia directly monitor the functional state of synapses in vivo and determine the fate of ischemic terminals. J. Neurosci. 29, 3974–3980.

Webb, S.J., Nalty, T., Munson, J., Brock, C., Abbott, R., Dawson, G., 2007. Rate of head circumference growth as a function of autism diagnosis and history of autistic regression. J. Child Neurol. 22, 1182–1190.

Zimmerman, A.W., Jyonouchi, H., Comi, A.M., Connors, S.L., Milstien, S., Varsou, A., Heyes, M.P., 2005. Cerebrospinal fluid and serum markers of inflammation in autism. Pediatr. Neurol. 33, 195–201.